JOURNAL OF AGRICULTURAL AND FOOD CHEMISTRY

Determination of Spore Inactivation during Thermal and Pressure-Assisted Thermal Processing Using FT-IR Spectroscopy

ANAND SUBRAMANIAN, JUHEE AHN,† V. M. BALASUBRAMANIAM, AND LUIS RODRIGUEZ-SAONA*

Department of Food Science and Technology, Ohio State University, 2015 Fyffe Court, Columbus, Ohio 43210

The efficacy of microbial inactivation techniques is currently tested using time-consuming and labor-intensive plate count methods, which are the principal rate-limiting steps in developing inactivation kinetic parameters for alternative food processing technologies. Fourier transform infrared (FT-IR) spectroscopy combined with multivariate analysis was used to quantify viable spores and identify some biochemical changes in samples treated by autoclaving, pressure-assisted thermal processing (PATP), and thermal processing (TP). Spore suspensions (~10^9 CFU/mL) of *Bacillus amyloliquefaciens* TMW 2.479 Fad 82, *B. amyloliquefaciens* TMW 2.482 Fad 11/2, *B. sphaericus* NZ 14, *B. amyloliquefaciens* ATCC 49764, and *Clostridium tyrobutyricum* ATCC 25755 were treated by PATP (121 °C and 700 MPa) for 0, 10, 20, and 30 s and by TP (121 °C) for 0, 10, 20, and 30 s. The concentrations of spores in treated samples were determined by plating (reference method). Models developed using partial least-squares regression (PLSR) for predicting spore levels in treated samples had correlation coefficients (r) of >0.99 and standard errors of cross-validation ranging between $10^{0.2}$ and $10^{0.5}$ CFU/mL. Changes in dipicolinic acid (DPA) and secondary structure of proteins were found to occur during inactivation of spores by PATP and TP. FT-IR spectroscopy could rapidly estimate viable bacterial spore levels in PATP- and TP-treated spore suspensions, providing an accurate analytical tool for monitoring the efficacy of sterilization techniques in inactivating spore-forming microorganisms.

KEYWORDS: Fourier transform infrared spectroscopy; multivariate analysis; spore viability; pressure-assisted thermal processing; thermal processing

INTRODUCTION

The food industry is interested in advanced sterilization processing methods that have a minimal thermal impact on low-acid foods. Among the technologies investigated are ohmic heating, microwave heating, and pressure-assisted thermal processing (PATP). Thermal sterilization inactivates bacterial spores of public health significance, but the typical high temperatures and long heating times used can adversely affect the nutritional and sensory characteristics of most foods. Therefore, less detrimental alternative processing technologies such as PATP are desirable (*1*, *2*). PATP involves processing foods under a combination of pressure (600−900 MPa) and temperature (90−121 °C) (*3*). Compared to thermal processing (TP), PATP offers various advantages including rapid destruction of microorganisms, rapid and uniform increase in temperature of treated samples, less quality loss due to reduced thermal impact, and shelf life extension of the product (*1*−*3*). PATP is being widely researched for potential applications in low-acid products such as soups, egg products, coffee, tea, and mashed potatoes. Limited studies have addressed PATP spore inactivation over a range of pressure and temperature conditions (*3*−*5*). Microbiological safety of PATP must be ensured before it can be commercially applied for food processing.

Traditional microbiological plating techniques are time-consuming and the principal rate-limiting step in developing microbial inactivation models. Hence, there is a significant need for rapid, high-throughput, and reliable methods of determination of microbial inactivation. Fourier transform infrared (FT-IR) spectroscopy, because of its inherent advantages such as simplicity, rapidity, and high sensitivity and throughput, has been proposed as an alternative technique for the rapid characterization of microorganisms by many researchers over the past few decades (*6*−*8*). FT-IR spectroscopy produces specific spectral patterns according to the cellular constituents (*9*), which enables strain-level discrimination and identification of whole microbial cells. Proteins, lipids, polysaccharides, nucleic acids, and other biomolecules present in the cells provide

* To whom corrspondence should be addressed. Phone: 614-292-3339. Fax: 614-292-0218. E-mail: rodriguez-saona.1@osu.edu.
† Current address: Department of Biomaterials Engineering, School of Bioscience and Biotechnology, Kangwon National University, Chuncheon 200-701, South Korea.

10.1021/jf0622174 CCC: $33.50
Published on Web 12/08/2006

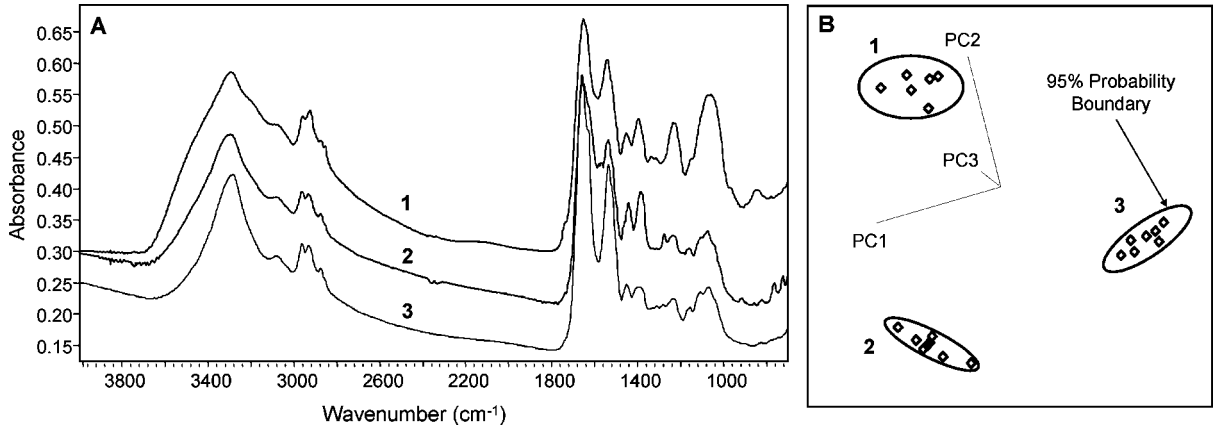

Figure 1. SIMCA class projections illustrating the separation that exists between vegetative cells, untreated spores, and autoclaved spores of *Bacillus subtilis*. (**A**) Fourier transform mid-infrared spectra (4000–700 cm^{-1}) of *B. subtilis* using a three-bounce AMTIR–ATR crystal. (**B**) SIMCA class projections of transformed (Savitzky–Golay second derivative, five-point window) and vector-length-normalized mid-infrared spectra (1800–900 cm^{-1}) of *B. subtilis*. 1, vegetative cells; 2, live spores; and 3, autoclaved spores.

Table 1. Assignment of Bands in the FT-IR Spectra of Bacterial Spores

frequency (cm^{-1})	functional group assignment[a]
~1655	amide I band of α-helical structure of secondary proteins
~1637	amide I band of β-pleated sheets of secondary proteins
~1626	amide I band of β-pleated sheets of secondary proteins (shifted because of autoclaving)
~1616	stretching bands of COO^- group of DPA-Ca chelate
~1570	C–N vibrations of the DPA ring
~1535	amide II polypeptide structures
~1442	bands of acid peptides (*22*)/DPA pyridine ring vibration (*18*, *21*)
~1410	C–O–H in-plane bending of lipids, carbohydrates, and proteins
~1378	stretching bands of COO^- group of DPA–Ca chelate
~1280	amide III bands of proteins (*9*, *12*)/DPA band (*19*)

[a] Summarized from refs *7*, *9*, *12*, *18*, *21*, *22*, *24*, *29*, and *30*.

reproducible biochemical fingerprints that are unique for different bacteria. Application to the data of mathematical transformations such as derivatization and improved chemometric methods such as principle component analysis for cluster analysis has diversified the application of FT-IR into various fields of study (*10*). Moreover, advances in FT-IR spectroscopic instrumentation have made this technology ideal for large-volume, high-throughput, rapid screening and identification of potential microbial pathogens.

Extensive research has been conducted by many groups in the past decade on the application of FT-IR spectroscopy in the detection, identification, and characterization of microorganisms (*11*−*16*). A detailed list of applications of FT-IR spectroscopy in the discrimination, classification, and identification of microorganisms has been compiled by Mariey et al. (*17*). FT-IR spectroscopy has also been successfully employed by some researchers for the characterization of bacterial spores (*7*, *18*−*22*). However, few studies have been performed on the application of FT-IR spectroscopy to the quantification of biological agents such as bacteria (*23*−*25*). To the best of our knowledge, no research has been published on the use of FT-IR spectroscopy for the quantification of bacterial spores, which are a major concern from the food and biosecurity points of view.

Application of FT-IR spectroscopy to the rapid quantification of bacterial spores can help in the development of valuable predictive inactivation and growth models that can be used to validate alternative food processing technologies such as PATP. Apart from quantitative analysis, FT-IR spectroscopy can also provide chemical information that would allow monitoring of subtle compositional changes in the spore structure to predict spore inactivation and elucidate the mechanism of spore inactivation by thermal and nonthermal treatments. The objective of this study was to develop a simple, rapid, and reliable technique using FT-IR spectroscopy and multivariate analysis to predict viable spore concentrations in samples treated by PATP and TP.

MATERIALS AND METHODS

Bacterial Strains and Spore Production. On the basis of previous studies on combined pressure-thermal resistance of various spore-forming surrogate organisms conducted by Ahn et al. (*26*), *Bacillus amyloliquefaciens* TMW 2.479 Fad 82, TMW 2.482 Fad 11/2, and ATCC 49764 (high resistance to pressure); *Bacillus sphaericus* NZ 14 (moderate resistance to pressure); and *Clostridium tyrobutyricum* ATCC 25755 (low resistance to pressure) were chosen for investigation. *Bacillus amyloliquefaciens* TMW 2.479 Fad 82 and *B. amyloliquefaciens* TMW 2.482 Fad 11/2, originally isolated from ropy bread, were provided by M. Gänzle, Lehrstuhl für Technische Mikrobiologie, Technische Universität München (Freising, Germany). *B. amyloliquefaciens* ATCC 49764 and *C. tyrobutyricum* ATCC 25755 were purchased from American Type Culture Collection (Manassas, VA). *Bacillus sphaericus* NZ 14 was provided by R. Robertson, Fonterra Research Centre (Palmerston North, New Zealand). Spore suspensions were prepared in deionized water, following the procedure described by Rajan et al. (*3*). The approximate concentration of spores in the suspensions was determined to be ~10^9 CFU/mL by plating on reinforced clostridial agar (RCA) or tryptic soy agar (TSA; Fisher Scientific, Pittsburgh, PA). Both media were supplemented with 10 ppm of magnesium sulfate.

Preparation of Spore Samples. Aliquots (1.2 mL) of the aqueous spore suspensions of *B. amyloliquefaciens* TMW 2.479 Fad 82, *B. amyloliquefaciens* TMW 2.482 Fad 11/2, and *C. tyrobutyricum* ATCC 25755 were prepared according to a technique described by Rajan et al. (*3*) and Ahn et al. (*26*). Pouches made from sterile filter bags (01-002-57, Fisher Scientific) were used as sample holders. The packaged spore samples were then placed in a sample carrier consisting of a 10-mL-capacity polypropylene syringe (model 309604; Becton, Dickinson and Company, Franklin Lakes, NJ) covered with two layers of insulating material (model 09-356; Fisher Scientific). Water was used as the pressure-transmitting fluid within the syringe.

Autoclaving of Endospores. The effects of autoclaving on the spores were investigated using *Bacillus subtilis* OSU 494. A spore suspension of *B. subtilis* was autoclaved for 15 min at 0.103 MPa gauge pressure and 121 °C temperature. Spectra of the autoclaved spore suspension

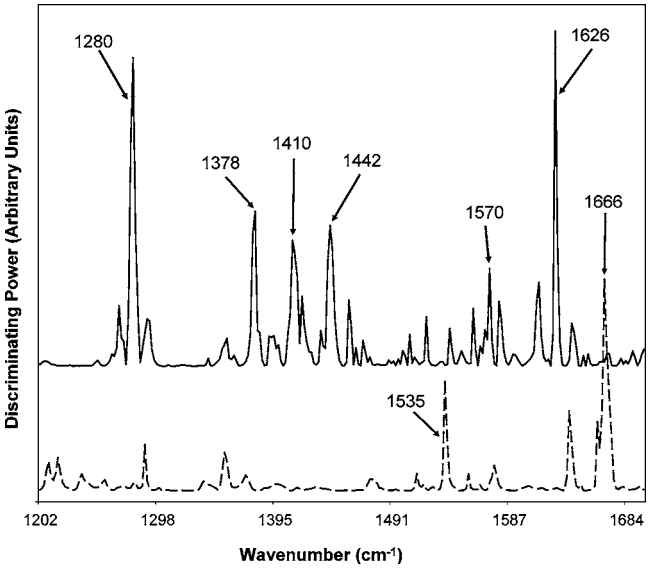

Figure 2. Discriminating power for classification of vegetative cells, untreated spores, and autoclaved spores of *Bacillus subtilis*. (—) Prominent bands in the discrimination of untreated spores and autoclaved spores of *B. subtilis*. (– – –) Prominent bands in the discrimination of autoclaved spores and vegetative cells of *B. subtilis*. Samples were prepared in distilled water and measured by ATR on an AMTIR surface.

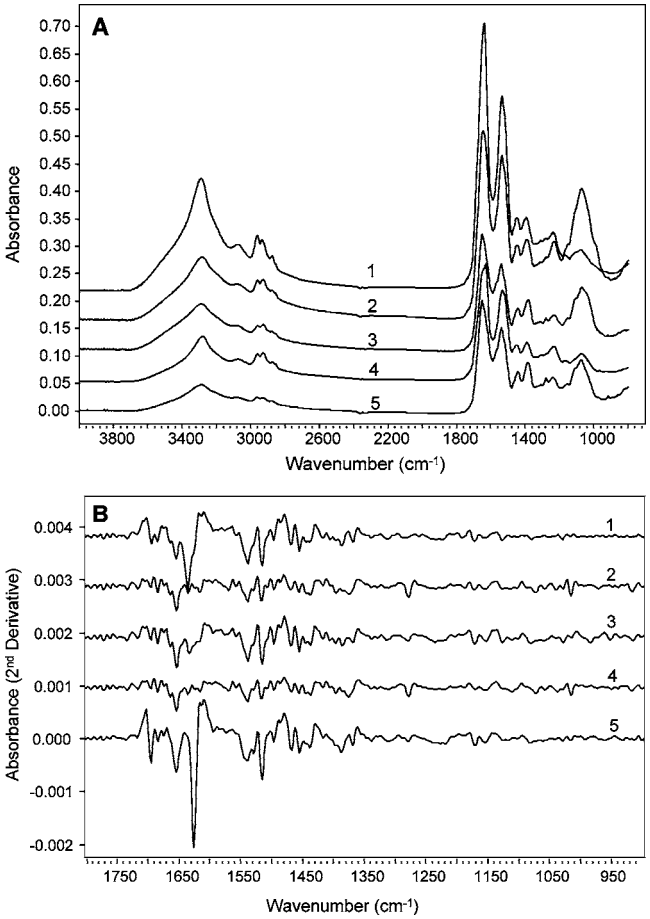

Figure 3. Fourier transform mid-infrared spectra of *Bacillus* and *Clostridia* spores prepared in distilled water and measured on a three-bounce AMTIR–ATR crystal. (**A**) Mid-infrared absorbance spectra of spores in the 4000–700 cm^{-1} range. (**B**) Transformed (Savitzky–Golay second derivative, five-point window) mid-infrared spectra of spores in the range of 1800–900 cm^{-1}. 1, *Bacillus sphaericus* NZ 14; 2, *B. amyloliquefaciens* ATCC 49764; 3, *B. amyloliquefaciens* Fad 82; 4, *C. tyrobutyricum* ATCC 25755; and 5, *B. amyloliquefaciens* Fad 11/2.

were obtained as described later and compared with those of vegetative cells and untreated spores of *B. subtilis*.

Pressure-Assisted Thermal Processing of Spore Suspension. Pressure-assisted thermal processing experiments were conducted using custom-fabricated high-pressure equipment (PT-1, Avure Technologies, Kent, WA), as described by Rajan et al. (*3*) and Ahn et al. (*26*). The packaged spore samples were subjected to PATP at a temperature of 121 °C and a pressure of 700 MPa for 0 (come-up time or 0-s holding time at 121 °C and 700 MPa), 10, 20, and 30 s. The come-up time (time to attain the set temperature and pressure) of the equipment was 30 s. An untreated suspension was used as the control. The treated spores were plated in RCA (for *Clostridia*) or TSA (for *Bacillus*) and counted to determine the viable spore concentration.

Thermal Treatment of Spore Suspension. Thermal inactivation of *B. amyloliquefaciens* TMW 2.479 Fad 82 and TMW 2.482 Fad 11/2 spores was carried out using custom-fabricated aluminum tubes, as described by Rajan et al. (*3*). Aluminum tubes containing aqueous spore suspensions were submerged simultaneously into a 28-L circulating oil bath maintained at 121 °C. The come-up time was approximately 3.0 min. A set of tubes was removed from the bath immediately after the come-up time, and the remaining tubes were removed after holding times of 10, 20, and 30 s. After removal from the bath, the tubes were immediately immersed into an ice−water bath to avoid further inactivation. An untreated spore suspension was used as the control. Spores surviving the thermal treatment were enumerated by plating on TSA.

FT-IR Spectroscopy. Autoclaved, PATP-treated, TP-treated, and untreated samples were stored under refrigerated conditions and analyzed within 2 days. Aliquots (200 μL) of the samples were centrifuged at 13000 rpm for 3 min. The deposited pellet of spores was washed with distilled water (100 μL), centrifuged, and resuspended in 50 μL of distilled water. Aliquots (10 μL) of the prepared sample were placed on the MIRacle attenuated total reflectance (ATR) accessory with a three-bounce AMTIR crystal (Pike Technologies, Madison, WI) and vacuum-dried to form a thin film. In a three-bounce crystal, infrared light is bounced on the sample three times, increasing the absorption and thereby increasing the signal intensity. Infrared spectra were recorded between 4000 and 800 cm^{-1} at a resolution of 8 cm^{-1} on an FTS Excalibur 3500GX FTIR spectrometer (Digilab, Randolph, MA) equipped with a PERMAGLOW mid-IR source, an extended-range KBr beam splitter, and a deuterated triglycine sulfate detector. Interferograms of the samples recorded by the data collection software (Win IR Pro version 4.0, Digilab Inc., Randolph, MA) were Fourier-transformed to obtain a single-beam spectrum and ratioed against the background to obtain the absorbance spectrum. To improve the signal-to-noise ratio, 128 scans were co-added for each spectrum. For each of the two independently produced and treated spore samples, between 3 and 5 spectra were collected, resulting in a total of 6−10 spectra per sample per treatment time.

Multivariate Analyses. Multivariate analyses of the data were carried out using commercial Pirouette (v3.11, Infometrix Inc., Woodville, WA) comprehensive chemometrics modeling software. The spectra were imported as GRAMS (.spc) files into Pirouette, mean-centered, transformed into their second derivatives using a Savitzky−Golay polynomial filter (five-point window), and vector-length normalized. Differentiation of vegetative cells and untreated and autoclaved spores of *B. subtilis* was carried out using classification analysis based on SIMCA (soft independent modeling by class analogy) (*13*). The data were projected onto principal component axes to visualize clustering of the three classes (vegetative cells, untreated spores, and autoclaved spores). The spectral regions influencing the classification of the three classes were determined from the measure of variable importance (discriminating power). For monitoring of the inactivation of spores during PATP and TP, the data were analyzed by partial least-squares regression (PLSR). Using specific fingerprint spectral information and the spore count determined by plating (reference method), multivariate analysis based on PLSR was used to model the relationships

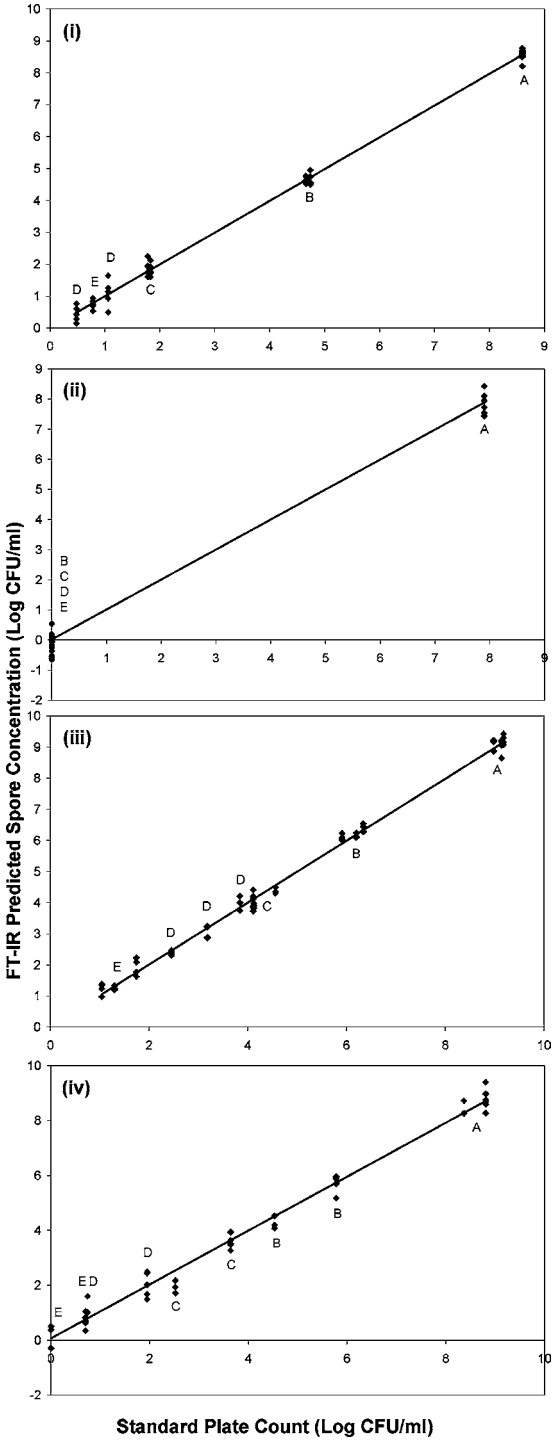

Figure 4. Partial least-squares regression model for *Bacillus* and *Clostridia* spores treated by pressure-assisted thermal processing (121 °C; 700 MPa; 0-, 10-, 20-, and 30-s holding times) and thermal processing (121 °C; 0-, 10-, 20-, and 30-s holding times). Savitzky–Golay second derivative transformation was used for multivariate analysis. (**i**) *B. amyloliquefaciens* Fad 82 treated by PATP, (**ii**) *C. tyrobutyricum* treated by PATP, (**iii**) *B. amyloliquefaciens* Fad 82 treated by TP, and (**iv**) *B. amyloliquefaciens* Fad 11/2 treated by TP. (A) Control (untreated), (B) 0 s (come-up time), (C) 10 s, (D) 20 s, and (E) 30 s.

between large numbers of dependent variables to predict the viable spore concentrations in the samples. PLSR models with cross-validation were developed to predict the viable spore concentrations of the five strains of spores mentioned earlier during PATP and TP. A nonlinear iterative partial least-squares (NIPALS) algorithm was employed.

RESULTS AND DISCUSSION

FT-IR spectra of the samples were collected between the frequencies 4000 to 800 cm^{-1}, using a three-bounce AMTIR crystal on an ATR accessory. The raw spectra were transformed into their second derivatives for analysis to remove the baseline shifts, improve the peak resolution, and reduce the variability between replicates (*27*).

Effect of Autoclaving on Endospores. The capability of FT-IR spectroscopy combined with multivariate analysis to differentiate *B. subtilis* spores and vegetative cells was investigated. The sample preparation method yielded high-quality spectra with consistent absorbance values. Resuspension of spore pellets from centrifugation in water, followed by drying on an ATR crystal, resulted in the formation of a thin and uniform film on the crystal. This allowed for the collection of spectra from vegetative cells and untreated and autoclaved spores of *B. subtilis* that showed distinct spectral features. Visual comparison of the raw spectra showed numerous differences, especially between 1800 and 1200 cm^{-1} (**Figure 1A**) associated with specific bacterial functional groups (**Table 1**). Soft independent modeling of class analogy (SIMCA) was used to develop classification algorithms based on principal component analysis (PCA) for each training set category. The PCA models for each class were developed by computing a small number of orthogonal variables (the principal components or PCs) that explained as much of the variation as possible between the samples in that class, preserving the relevant information and eliminating random variation (noise) (*28*). The SIMCA scores plot, a projection of the original data onto the principal components, allowed for the visualization of well-separated clustering among the three classes (vegetative cells, untreated spores, and treated spores) (**Figure 1B**).

The discriminating power allows for the identification of the frequencies that influence the differentiation of the classes in a SIMCA class projection. **Figure 2** shows a stacked plot of discriminating powers in differentiating untreated spores from autoclaved spores and autoclaved spores from vegetative cells of *B. subtilis*. Many spectral bands were involved in the differentiation of untreated spores from autoclaved spores (**Table 1**), most of which were associated with DPA and the secondary structure of proteins. Amide I of β-pleated sheet structures of secondary protein has been reported to absorb in the 1637 cm^{-1} region (*7*, *24*). Structural modifications such as denaturation and subsequent aggregation during autoclaving have been reported to cause a species-dependent shift in the amide I band from 1637 to ~1630 cm^{-1} (*19*). Therefore, the band at 1626 cm^{-1}, which was found to play a vital role in differentiating autoclaved spores of *B. subtilis* from untreated spores, could be attributed to a spectral shift caused by the structural modifications of β-sheets of amide I during autoclaving. Additionally, loss of band intensity at ~1570 and ~1279 cm^{-1}, associated with loss of DPA, has also been reported to occur during autoclaving (*19*). The frequencies corresponding to DPA, 1280, 1378, 1442, 1570, and 1616 cm^{-1}, were very influential in the discrimination of untreated spores from autoclaved spores (**Figure 2**). However, none of these bands had a significant effect on the discrimination of autoclaved spores from vegetative cells of *B. subtilis*. This confirms the release of DPA and its derivatives from the spores during inactivation by autoclaving.

In the discrimination of autoclaved spores from vegetative cells, major differences were due to the spectral frequencies 1666 and 1535 cm^{-1}, which can be attributed to amide I and amide II vibrations, respectively (**Figure 2**). Differentiation of vegetative cells, untreated spores, and autoclaved spores, shown in **Figure 1B**, revealed that bands at ~1280, ~1410, and ~1442

Table 2. Partial Least-Squares Model Parameters for *Bacillus* and *Clostridium* Spores

	PATP[a]			TP[b]		
bacterial strain	SECV[c]	correlation coefficient (r)	latent variables	SECV	correlation coefficient (r)	latent variables
B. amyloliquefaciens Fad 82	$10^{0.21}$	0.998	9	$10^{0.20}$	0.997	9
B. amyloliquefaciens Fad 11/2	$10^{0.21}$	0.998	11	$10^{0.36}$	0.993	11
B. amyloliquefaciens ATCC 49764	$10^{0.50}$	0.990	11			
B. sphaericus NZ 14	$10^{0.41}$	0.992	5			
C. tyrobutyricum ATCC 25755	$10^{0.25}$	0.997	8			

[a] Pressure-assisted thermal processing of the spore samples was carried out 0, 10, 20, and 30 s at 121 °C and 700 MPa. [b] Thermal processing the spore samples was carried out for 0, 10, 20, and 30 s at 121 °C. [c] Standard error of cross-validation.

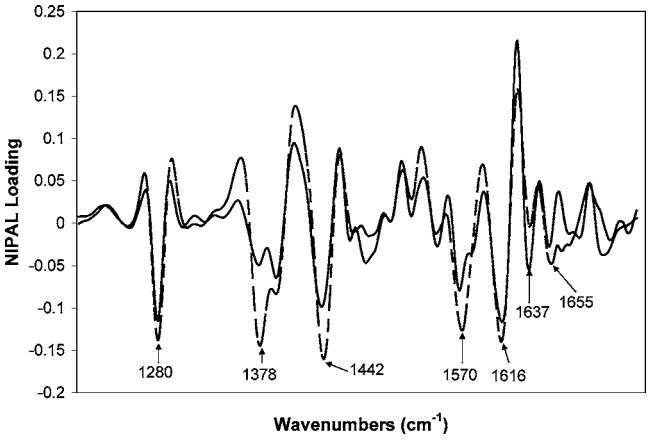

Figure 5. Factor 1 nonlinear iterative partial least-squares algorithm (NIPAL) loading for *Bacillus amyloliquefaciens* Fad 82. (—) Thermal processing and (– – –) pressure-assisted thermal processing.

cm^{-1} influenced the classification (discriminating power not shown). The structural modifications in the β-sheets of secondary proteins, corresponding to the band at $\sim$1626 cm^{-1}, was not highlighted as being important for the discrimination of untreated and autoclaved spores from vegetative cells. Also, absorption bands of DPA in the region from 3100 to 3600 cm^{-1} (deprotonated carboxylate form; *18*) did not affect the SIMCA classifications. These data clearly indicate that FT-IR spectroscopy combined with multivariate analysis can not only differentiate vegetative cells, untreated and autoclaved spores of *B. subtilis* but also elucidate some of the major biochemical differences among the three samples. Therefore, by monitoring biochemical changes in spores during PATP and TP, FT-IR spectroscopy can be used as a simple and rapid tool to determine bacterial spore inactivation.

PLSR Models for PATP-Treated Spores. Inactivation of *Bacillus amyloliquefaciens* Fad 82, *B. amyloliquefaciens* Fad 11/2, *B. amyloliquefaciens* ATCC 49764, *B. sphaericus* NZ 14, and *Clostridium tyrobutyricum* ATCC 25755 during PATP and TP was monitored using FT-IR spectroscopy. The FT-IR absorption spectra of the five strains of bacterial spores are shown in **Figure 3A**. The raw spectra of the five strains showed subtle differences in the region between 1800 and 900 cm^{-1}. The raw spectra were transformed into their second derivatives for quantitative analysis (**Figure 3B**).

For analysis, spores of all five bacterial strains were subjected to PATP (121 °C and 700 MPa) treatment for 0, 10, 20, and 30 s. The transformed spectra of these samples and the corresponding spore concentrations obtained from standard plate counts (reference technique) were used to develop PLSR models. The PLSR models for *B. amyloliquefaciens* Fad 82 and *C. tyrobutyricum* ATCC 25755, which were determined previously to be most and least resistant, respectively, to PATP (*26*), are shown in **Figure 4i** and **ii**, respectively. *Bacillus amyloliquefaciens* Fad 82 exhibited biphasic inactivation with a high inactivation rate at the beginning followed by reduced inactivation during extended pressure holding times. *Bacillus amyloliquefaciens* Fad 11/2 exhibited similar inactivation characteristics (data not shown). A reduction of approximately 7−8 logarithm units was observed in the spore population at the end of the 30-s PATP treatment (*3*). In contrast, *C. tyrobutyricum* was completely inactivated at the end of the come-up time (*26*). The reduction in concentration of >7 logarithm units observed during the come-up time can be attributed to the susceptibility of this strain to PATP. Samples treated for 0-, 10-, 20-, and 30-s holding times clustered together, indicating their similar chemical compositions. Hence, it can be concluded that, after inactivation of the spores, the pressure holding time did not cause any significant biochemical changes in the spores. *Bacillus amyloliquefaciens* ATCC 49764 and *B. sphaericus* NZ 14 exhibited moderate resistance to PATP, with *B. amyloliquefaciens* ATCC 29764 more resistant than *B. sphaericus* NZ 14. The PLSR model parameters for all five strains of bacterial spores are summarized in **Table 2**. All PLSR models exhibited excellent fits, with standard errors of cross-validation (SECV) ranging between $10^{0.21}$ and $10^{0.50}$ CFU/mL and coefficients of correlation (r) $\geq$0.99. The standard error of cross-validation is an estimate of the error expected when independent samples are predicted using the model.

PLSR Models for TP-Treated Spores. *B. amyloliquefaciens* Fad 82 and *B. amyloliquefaciens* Fad 11/2 were subjected to TP for 0, 10, 20, and 30 s at 121 °C. PLSR models developed using the transformed spectra and plate counts are shown in **Figure 4iii** and **iv**, respectively. As expected, both *B. amyloliquefaciens* Fad 82 and *B. amyloliquefaciens* Fad 11/2 were found to be resistant to TP. They were not inactivated completely even after 30 s of holding at 121 °C. PLSR models developed for TP-treated samples also exhibited excellent reliability. The standard error of cross-validation values for *B. amyloliquefaciens* Fad 82 and *B. amyloliquefaciens* Fad 11/2 were $10^{0.2}$ and $10^{0.36}$ CFU/mL, respectively. The coefficient of correlation was $\geq$0.99. The PLSR model parameters for the two strains are summarized in **Table 2**. These models clearly indicate that FT-IR spectroscopy combined with multivariate analysis can be used to develop reliable models for the rapid prediction of viable spore concentrations in samples treated by PATP and TP.

Changes in Spores during Inactivation. Between 5 and 11 factors (latent variables) were used in the development of the PLSR models for the five different spore strains. Each orthogonal factor is a set of various components (frequency regions) providing an optimal linear model in terms of predictivity. For

each of the strains, 2 or 3 factors explained ≥80% of the total differences between the samples treated for different processing times. For example, in developing the PLSR models for the inactivation of *B. amyloliquefaciens* Fad 82 by PATP and TP, a total of 9 factors were used. Factor 1 explained ~83% and ~77% of the differences in samples processed for different times by PATP and TP, respectively (**Figure 5**). The prominent components constituting factor 1 are summarized in **Table 1**. Some of the biochemical changes taking place during spore inactivation by PATP were found to be similar to those occurring during TP, although the intensities of these changes were different.

Conclusions. A novel application of FT-IR spectroscopy to the monitoring of bacterial spore inactivation in model systems during TP and PATP was demonstrated. The total time required for sample preparation and IR analysis was less than 15 min. The above results clearly indicate the potential of FT-IR spectroscopy for rapid analysis of bacterial spore samples. However, further development of the technique might be required before it can be applied to actual food systems, which are complex matrices of various components that can cause interference. FT-IR spectroscopy also elucidated some of the biochemical and structural changes taking place in the spores during inactivation by PATP and TP. Such information can be used in optimizing processing parameters to target specific compounds, which would, in turn, aid in rapid and effective sterilization. The rapid infrared spectroscopic technique proposed in this study can be a valuable tool to industry for analyzing the microbial quality of products, monitoring the effectiveness of processing and sanitation treatments, and improving quantitative risk analysis methods. With knowledge of the biochemical components contributing to the PATP and TP resistance of spores, FT-IR spectroscopy can also be used for the rapid screening of processing-resistant spores.

LITERATURE CITED

(1) Matser, A. M.; Krebbers, B.; van den Berg, R. W.; Bartels, P. V. Advantages of high pressure sterilization on quality of food products. *Trends Food Sci. Technol.* **2004**, *15*, 79−85.

(2) Raso, J.; Barbosa-Canovas, G. V. Nonthermal preservation of foods using combined processing techniques. *Crit. Rev. Food Sci. Nutr.* **2003**, *43*, 265−285.

(3) Rajan, S.; Ahn, J.; Balasubramaniam, V. M.; Yousef, A. E. Combined pressure−thermal inactivation kinetics of *Bacillus amyloliquefaciens* spores in egg patty mince. *J. Food Prot.* **2006**, *69*, 853−860.

(4) Margosch, D.; Ehrmann, M. A.; Ganzle, M. G.; Vogel, R. F. Comparison of pressure and heat resistance of *Clostridium botulinum* and other endospores in mashed carrots. *J. Food Prot.* **2004**, *67*, 2530−2537.

(5) Reddy, N. R.; Solomon, H. M.; Fingerhut, G. A.; Balasubramaniam, V. M.; Palaniappan, S. Inactivation of *Clostridium botulinum* type E spores by high pressure processing. *J. Food Saf.* **1999**, *19*, 277−288.

(6) Riddle, J. W.; Kabler, P. W.; Kenner, B. A.; Bordner, R. H.; Rockwood, S. W.; Stevenson, H. J. Bacterial identification by infrared spectrophotometry. *J. Bacteriol.* **1956**, *72*, 593−603.

(7) Naumann, D.; Helm, D.; Labischinski, H. Microbiological characterization by FT-IR spectroscopy. *Nature* **1991**, *351*, 81−82.

(8) Helm, D.; Labischinski, H.; Schallehn, G.; Naumann, D. Classification and identification of bacteria by Fourier-transform infrared spectroscopy. *J. Gen. Microbiol.* **1991**, *137*, 69−79.

(9) Helm, D.; Naumann, D. Identification of some bacterial cell components by FT-IR spectroscopy. *FEMS Microbiol. Lett.* **1995**, *126*, 75−80.

(10) Rodriguez-Saona, L. E.; Khambaty, F. M.; Fry, F. S.; Calvey, E. M. Rapid detection and identification of bacterial strains by Fourier transform near-infrared spectroscopy. *J. Agric. Food Chem.* **2001**, *49*, 574−579.

(11) Lamprell, H.; Mazerolles, G.; Kodjo, A.; Chamba, J. F.; Noel, Y.; Beuvier, E. Discrimination of *Staphylococcus aureus* strains from different species of *Staphylococcus* using Fourier transform infrared (FTIR) spectroscopy. *Int. J. Food Microbiol.* **2006**, *108*, 125−129.

(12) Yu, C.; Irudayaraj, J. Spectroscopic characterization of microorganisms by Fourier transform infrared microspectroscopy. *Biopolymers* **2005**, *77*, 368−377.

(13) Baldauf, N. A.; Rodriguez-Romo, L. A.; Yousef, A. E.; Rodriguez-Saona, L. E. Differentiation of selected *Salmonella enterica* serovars by Fourier transform mid-infrared spectroscopy. *Appl. Spectrosc.* **2006**, *60*, 592−598.

(14) Whittaker, P.; Mossoba, M. M.; Al-Khaldi, S.; Fry, F. S.; Dunkel, V. C.; Tall, B. D.; Yurawecz, M. P. Identification of foodborne bacteria by infrared spectroscopy using cellular fatty acid methyl esters. *J. Microbiol. Methods* **2003**, *55*, 709−716.

(15) Oberreuter, H.; Seiler, H.; Scherer, S. Identification of coryneform bacteria and related taxa by Fourier-transform infrared (FT-IR) spectroscopy. *Int. J. Syst. Evol. Microbiol.* **2002**, *52*, 91−100.

(16) Beattie, S. H.; Holt, C.; Hirst, D.; Williams, A. G. Discrimination among *Bacillus cereus*, *B. mycoides* and *B. thuringiensis* and some other species of the genus *Bacillus* by Fourier transform infrared spectroscopy. *FEMS Microbiol. Lett.* **1998**, *164*, 201−206.

(17) Mariey, L.; Signolle, J. P.; Travert, A. J. Discrimination, classification, identification of microorganisms using FTIR spectroscopy and chemometrics. *Vib. Spectrosc.* **2001**, *26*, 151−159.

(18) Perkins, D. L.; Lovell, C. R.; Bronk, B. V.; Setlow, B.; Setlow, P. Fourier transform infrared reflectance microspectroscopy study of *Bacillus subtilis* engineered without dipicolinic acid: The contribution of calcium dipicolinate to the mid-infrared absorbance of *Bacillus subtilis* endospores. *Appl. Spectrosc.* **2005**, *59*, 893−896.

(19) Perkins, D. L.; Lovell, C. R.; Bronk, B. V.; Setlow, B.; Setlow, P.; Myrick, M. L. Effects of autoclaving on bacterial endospores studied by Fourier transform infrared microspectroscopy. *Appl. Spectrosc.* **2004**, *58*, 749−753.

(20) Thompson, S. E.; Foster, N. S.; Johnson, T. J.; Valentine, N. B.; Amonette, J. E. Identification of bacterial spores using statistical analysis of Fourier transform infrared photoacoustic spectroscopy data. *Appl. Spectrosc.* **2003**, *57*, 893−899.

(21) Goodacre, R.; Shann, B.; Gilbert, R. J.; Timmins, E. M.; McGovern, A. C.; Alsberg, B. K.; Kell, D. B.; Logan, N. A. Detection of the dipicolinic acid biomarker in *Bacillus* spores using Curie-point pyrolysis mass spectrometry and Fourier transform infrared spectroscopy. *Anal. Chem.* **2000**, *72*, 119−127.

(22) Cheung, H. Y.; Cui, J.; Sun, S. Real-time monitoring of *Bacillus subtilis* endospore components by attenuated total reflection Fourier-transform infrared spectroscopy during germination. *Microbiology* **1999**, *145*, 1043−1048.

(23) Gupta, M. J.; Irudayaraj, J.; Debroy, C. Spectroscopic quantification of bacteria using artificial neural networks. *J. Food Prot.* **2004**, *67*, 2550−2554.

(24) Yu, C.; Irudayaraj, J.; Debroy, C.; Schmilovtich, Z.; Mizrach, A. Spectroscopic differentiation and quantification of microorganisms in apple juice. *J. Food Sci.* **2004**, *69*, S268−S272.

(25) Oberreuter, H.; Mertens, F.; Seiler, H.; Scherer, S. Quantification of micro-organisms in binary mixed populations by Fourier transform infrared (FT-IR) spectroscopy. *Lett. Appl. Microbiol.* **2000**, *30*, 85−89.

(26) Ahn, J.; Balasubramaniam, V. M.; Yousef, A. E. Inactivation kinetics of selected aerobic and anaerobic bacterial spores by pressure-assisted thermal processing. *Int. J. Food Microbiol.* **2006**, in press.

(27) Kansiz, M.; Heraud, P.; Wood, B.; Burden, F.; Beardall, J.; McNaughton, D. Fourier transform infrared microspectroscopy and chemometrics as a tool for the discrimination of cyanobacterial strains. *Phytochemistry* **1999**, *52*, 407−417.

(28) Mark, H. Data analysis: Multilinear regression and principal component analysis. In *Handbook of Near-Infrared Analysis*; Burns, D. A., Ciurczak, E. W., Eds.; Taylor and Francis: New York, 2001; pp 129−184.

(29) Naumann, D. Infrared spectroscopy in microbiology In *Encyclopedia of Analytical Chemistry*; Meyers, R. A., Ed.; John Wiley and Sons: Chichester, U.K., 2000; pp 102−131.

(30) Maquelin, K.; Kirschener, C.; Choo-Smith, L. P.; van den Braak, N.; Endtz, H. Ph.; Naumann, D.; Puppels, G. J. Identification of medically relevant microorganisms by vibrational spectroscopy. *J. Microbiol. Methods* **2002**, *51*, 255−271.

Received for review August 2, 2006. Revised manuscript received October 3, 2006. Accepted October 30, 2006. We thank the National Science Foundation I/UCRC and the Center for Advanced Processing and Packaging Studies for funding this project.

JF0622174